Calhoun: The NPS Institutional Archive
DSpace Repository

Theses and Dissertations 1. Thesis and Dissertation Collection, all items

1953

A broad band bi-directional coupler with tight coupling and high directivity

Eidson, Robert Ansel

Monterey, California: U.S. Naval Postgraduate School

http://hdl.handle.net/10945/13975

Downloaded from NPS Archive: Calhoun

Calhoun is the Naval Postgraduate School's public access digital repository for research materials and institutional publications created by the NPS community. Calhoun is named for Professor of Mathematics Guy K. Calhoun, NPS's first appointed -- and published -- scholarly author.

Dudley Knox Library / Naval Postgraduate School
411 Dyer Road / 1 University Circle
Monterey, California USA 93943

http://www.nps.edu/library

A BROAD BAND BI-DIRECTIONAL COUPLER WITH TIGHT COUPLING AND HIGH DIRECTIVITY

ROBERT ANSEL EIDSON

1953

Library
U. S. Naval Postgraduate School
Monterey, California

17-56

A BROAD BAND BI-DIRECTIONAL COUPLER WITH TIGHT COUPLING AND HIGH DIRECTIVITY

-

R. A. Eidson

Library
U. S. Naval Postgraduate School
Monterey, California

A BROAD BAND BI-DIRECTIONAL COUPLER WITH TIGHT COUPLING AND HIGH DIRECTIVITY

by

Robert Ansel Eidson,
Lieutenant, United States Navy

Submitted in partial fulfillment
of the requirements
for the degree of

MASTER OF SCIENCE

United States Naval Postgraduate School
Monterey, California
1953

E27

This work is accepted as fulfilling
the thesis requirements for the degree of
MASTER OF SCIENCE
IN
ENGINEERING ELECTRONICS

from the
United States Naval Postgraduate School.

PREFACE

A directional coupler is an electromagnetic device by which the magnitude of the voltage incident on and reflected by a load can be monitored. Since broad band operation is becoming a requirement for most microwave systems, the power measuring device must also become broad band. This paper deals with the design and development considerations of such a broad band bi-directional coupler.

This work is an outgrowth of a need for such a coupler in a Swept Frequency Oscillator System currently under development at Dalmo-Victor Company, San Carlos, California. The actual bi-directional coupler developed at Dalmo-Victor from the theory to be presented here, substantiates this method as a practical means of broad band directional coupler design.

The theory employed is not original. It is primarily the result of correlating and applying the work of several outstanding men in the electromagnetic field. Their contributions are noted throughout the body of this paper.

My sincere thanks to Professors C. E. Menneken and W. M. Bauer who as first and second readers contributed materially to this thesis by their helpful suggestions and criticisms.

R. A. Eidson

TABLE OF CONTENTS

	Page
CERTIFICATE OF APPROVAL	i
PREFACE	ii
LIST OF ILLUSTRATIONS	iv
TABLE OF SYMBOLS AND ABBREVIATIONS	v
CHAPTER	
I. INTRODUCTION	1
1. Summary	
2. Definitions	
3. Possible Uses	
4. Comparison with Slotted Lines and Hybrids	
II. DESIGN CONSIDERATIONS	8
1. General	
2. Coupling	
3. Directivity	
III. THEORETICAL DESIGN	16
IV. EXPERIMENTAL RESULTS	26
V. CONCLUSION	29
1. General	
2. Coupling	
3. Directivity	
BIBLIOGRAPHY	33
APPENDIX A	34
APPENDIX B	37

LIST OF ILLUSTRATIONS

Page
1. Block diagram of Swept Frequency Oscillator System -2a-
2. Directional coupler definitions -2b-
3. Directivity of a bi-directional coupler -9a-
4. Coupling element taper -11a-
5. Constant coupling plate by Miller-Mumford -13a-
6. Tapered coupling plate by Miller-Mumford -13a-
7. Superimposition of Tchebyscheff coefficients by Barnett -19a-
8. Final Design of coupling plate -19b-
9. Wave guide dimensions -20a-
10. $F_A(\lambda_g)$ versus x_1 -22a-
11. $F_A(\lambda_g)$ versus λ_g -23a-
12. Photograph of directional coupler -26b-
13. Test bench set-up -26a-
14. Theoretical and actual coupling curves -26c-
15. The technique used for measuring directivity -26d-
16. Theoretical and actual directivity curves. -28a-

TABLE OF SYMBOLS AND ABBREVIATIONS

a	Large internal rectangular wave guide dimension.
A_n	Voltage coupling coefficient in the forward wave direction for the n^{th} hole.
A_T	Total voltage coupling coefficients for all n longitudinally distinct holes.
b	small internal rectangular wave guide dimension.
B_n	Voltage coupling coefficient in the backward wave direction for the n^{th} hole.
C	Coupling in decibels.
D	Directivity in decibels.
d_n	Diameter of the n^{th} longitudinally distinct coupling hole.
n	An integer from 1 to n, numbering the longitudinally distinct coupling holes.
2N	Total number of longitudinally distinct coupling holes.
r_n	Radius of the n^{th} longitudinally distinct coupling hole.
t	Thickness of the common plate between the main and auxiliary wave guide.
T_n	Tchebyscheff coefficient for the n^{th} longitudinally distinct coupling hole.
T_T	Total of Tchebyscheff coefficients of all n coupling holes.
VSWR	Voltage Standing Wave Ratio.
x,y,z	Large dimension (a) axis, small dimension (b) axis, and longitudinal axis of the wave guide, respectively.
x_1	Dimension in the direction of the x-axis from the internal side wall to the center of a coupling hole. A constant for all n holes.

z_o	A design parameter which determines the width of the suppression band of a Tchebyscheff array.
Z_o	Characteristic impedence.
z_1	Dimension in the direction of the z-axis from the center of one coupling hole to the center of the next. A constant for all n holes.
α_E	Attenuation coefficient for the E field which compensates for the finite "t" in a wave guide coupler.
α_H	Attenuation coefficient for the H-field which compensates for the finite "t" in a wave guide coupler.
β	Wave number equal to $2\pi/\lambda_g$
Γ	Voltage coefficient of reflection.
λ_g	Guide Wave-length
λ_o	Free space wave-length
ρ	Geometric factor depending on the radius of a coupling hole and the thickness, t.

CHAPTER I

INTRODUCTION

1. Summary

Assuming that oscillators are available which will tune across the frequency band of a particular standard guide, the antenna load matching problem still confronts the radar engineer. Supposedly, broad band antennas have been designed. This should mean that there are no frequencies within the design bandwidth of the antenna at which high reflections occur. However, such antennas can only be tested at a finite number of selected frequencies unless a swept frequency oscillator system is used. The desired frequency bandwidth must be swept at a speed slow enough to give good resolution. This sweep is placed on the horizontal plates of an indicator. The swept frequency output is attached to a bidirectional coupler, whose main guide output goes to the antenna load. The two coupler outputs from the auxiliary guide proportional to the incident and reflected voltage of the load, are amplified through two separate logarithmic amplifiers. The logarithmic outputs go next to a difference amplifier from which the quotient of the reflected voltage to the incident voltage (coefficient or reflection) can be obtained. This quotient is related to the voltage standing wave ratio by the following well know formula:

$$VSWR = \frac{1+|\Gamma|}{1-|\Gamma|} \quad \text{where } |\Gamma| = \left|\frac{E_{ref}}{E_{inc}}\right| \qquad (1)$$

This quotient signal is placed on the vertical plates on the indicator whose face is calibrated with known values of VSWR. A block diagram of this system is illustrated in figure (1).

By use of this system, it is readily ascertained if there are any frequencies where a bad mismatch of antenna to transmission wave guide exist. The accuracy of the entire system depends upon the accuracy with which the two coupler output voltages can be obtained. The bi-directional coupler separates these two voltages and must therefore be carefully designed.

2. Definitions

Practically every term of the directional coupler theory is defined differently, depending upon the author. An attempt will be made (1) to define only those terms used in this paper, (2) to use the most common, and if possible, logical definitions, and (3) to adhere consistently to these definitions throughout the text.

Directional couplers are used in both coaxial and wave guide systems. Only wave guide directional couplers will be considered in this paper.

A directional coupler is a means of coupling electromagnetic waves from a main transmission guide to an auxiliary guide. It has the property of propagating the wave which is traveling in the auxiliary guide in the direction of the main guide wave (forward wave), while attenuating the wave in the auxiliary guide which is traveling in the direction opposite to the main guide wave (backward wave). See figure (2).

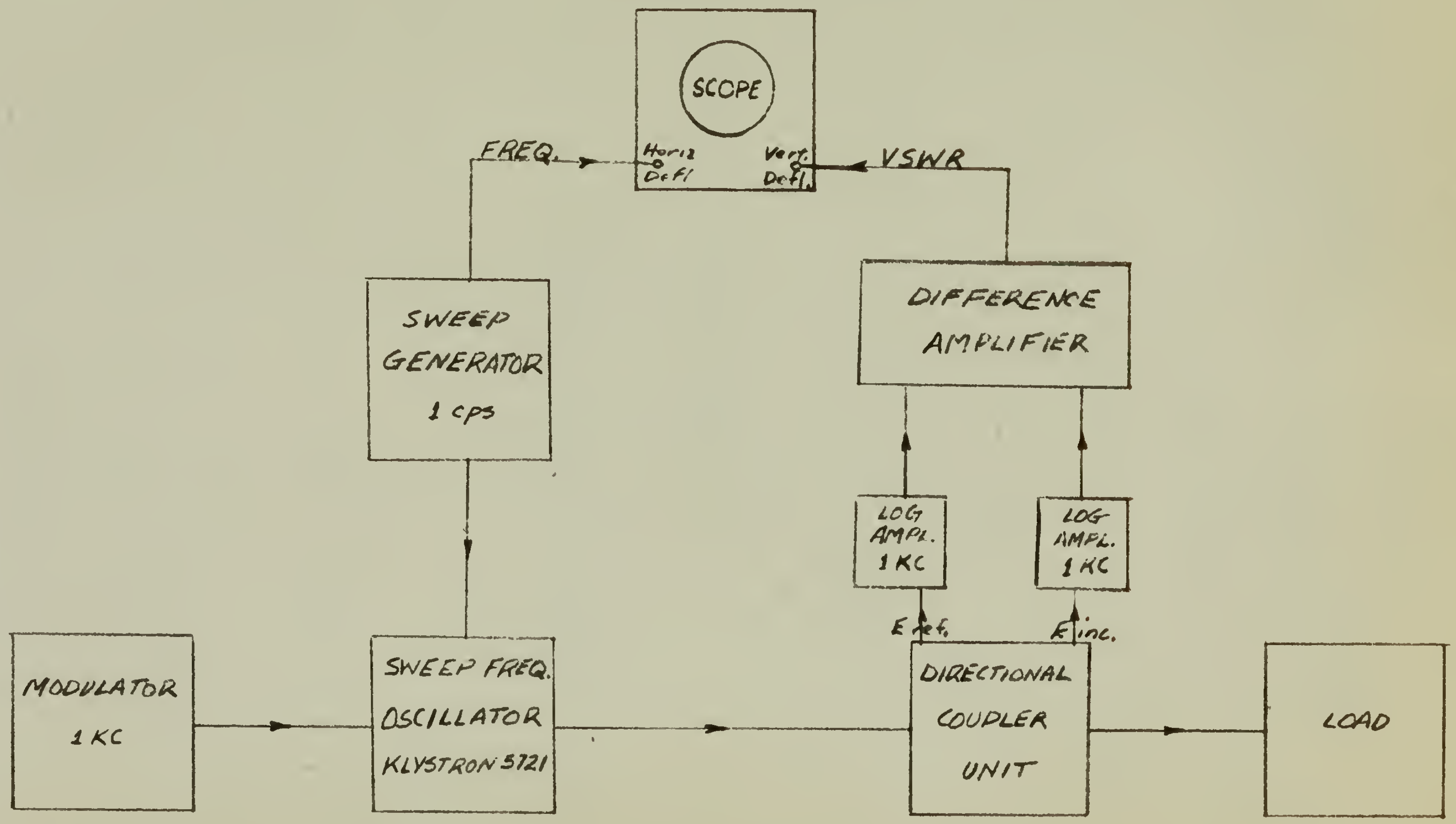

BLOCK DIAGRAM OF SWEPT FREQUENCY OSCILLATOR SYSTEM

FIGURE (1)

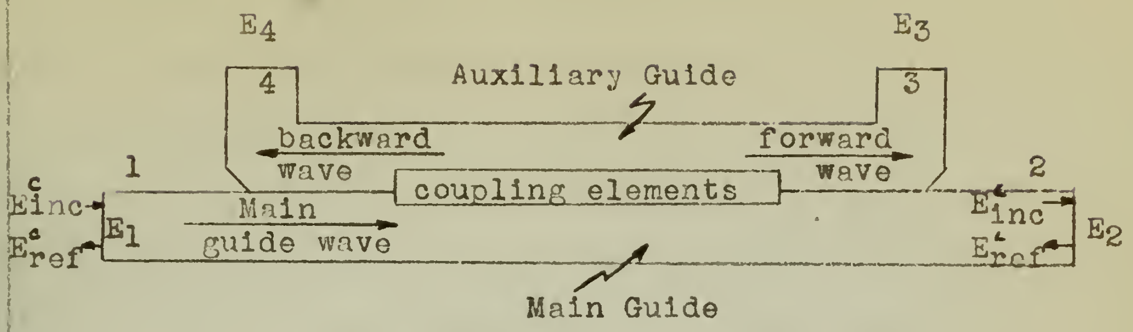

E_1, E_2, E_3, E_4-voltages across terminals 1,2,3,4.

(1) Coupling* in db = $C = 20 \log \frac{|E_3|}{|E_1|}$

(2) Directivity* in db = $D = 20 \log \frac{|E_3|}{|E_4|}$

(3) $|VSWR_{coupler}| = \frac{|E^{c}_{inc}| + |E^{c}_{ref}|}{|E^{c}_{inc}| - |E^{c}_{ref}|}$

$$|VSWR_{load}| = \frac{|E^{L}_{inc}| + |E^{L}_{ref}|}{|E^{L}_{inc}| - |E^{L}_{ref}|} = \frac{|E_3| + |E_4|}{|E_3| - |E_4|}$$

(4) $|\Gamma_L| = \frac{|E^{L}_{ref}|}{|E^{L}_{inc}|} \quad \frac{|E_4|}{|E_3|}$

* For measurement of these, all terminals must be perfectly matched.

DIRECTIONAL COUPLER DEFINITIONS

FIGURE (2)

It should be noted that directional couplers are symmetrical, which means they may be turned end for end with no effect on their external behavior. Referring to figure (2), it is seen that a voltage fed in at terminal 1 will divide between terminals 2 and 3, without appearing at terminal 4; while a voltage fed in at terminal 2 will divide between terminals 1 and 4 without appearing at terminal 3. In order for this statement to be strictly valid, the ideal conditions of perfectly matched terminations and perfect directivity must exist. However, this does serve to illustrate the principal properties of coupling and directivity of a directional coupler.

The auxiliary guide of the coupler usually has a single output with the other end terminated in its characteristic impedance, Z_o. The coupler therefore is capable of monitoring only the incident or the reflected wave at one time, depending upon its orientation in the wave guide system. It is of course possible to place two such couplers back to back* to monitor the incident and reflected wave at the same time. This gives isolation to each auxiliary output arm but doubles the length of the overall coupling system.

A bi-directional coupler has two outputs in the auxiliary guide. It has the advantages over the single-ended back to back coupling of being shorter and using common coupling elements for both outputs.

---

*When two single output directional couplers have their main guide connected in the wave guide system, with the coupler closest to the source positioned to monitor the incident voltage and the coupler closest to the load positioned to monitor the reflected voltage, they are said to be back to back.

However, these two arms have no isolation between them, which means that any reflection due to detector mismatch will introduce an error.

Coupling elements are the physical means of coupling power from the main to the auxiliary guide. They take the form of probes, loops, or apertures of any shape and size placed anywhere in either the large or small faces of the guide.

Coupling is one of two main terms which serve to specify the performance of a coupler. It is simply an indication of the amount of voltage coupled from the main to the auxiliary guide, as shown in figure (2), equation (1). Coupling is most commonly expressed in decibels as the ratio of the voltage delivered to the forward arm of the auxiliary guide to the voltage input to the coupler. Therefore, the coupling as defined here will always appear as a negative number of db. If a coupler is said to have -10db coupling, or just 10 db coupling, this means the voltage delivered to the forward arm of the auxiliary guide is 10 db below the input voltage.

Directivity is the second term which specifies the performance of a coupler. It represents the effectiveness with which a coupler attenuates a backward wave and propagates the forward wave in the auxiliary guide. It is most commonly given in db and is the ratio of the voltage of the forward wave to the voltage of the backward wave in the auxiliary guide. A coupler with 20 db directivity contains voltage in the backward wave which is 20 db below the voltage in the forward wave.

The VSWR of a coupler is often specified. However, when using Bethe's small hole theory for coupler design, the reflections of the coupler are usually so small compared with other reflections that they are insignificant.

Reflection Coefficient, $|\Gamma|$, is the ratio of the reflected voltage to the incident voltage.

Each of these last four terms are illustrated in figure (2) for a bi-directional coupler.

All future references to "couplers" will apply to directional couplers unless otherwise specified.

3. Possible Uses

Directional couplers have many uses in wave guide systems. Of these uses, the two most important are its use in monitoring a source, and its use in monitoring a load.

In monitoring a source, a coupler may monitor the power, the frequency, or the frequency spectrum of a transmitted pulse. As a power monitor, the coupler will also be an attenuator, the amount of attenuation required depending upon the sensitivity of the detection unit. With the attenuation a desirable feature, this type coupler will have loose coupling usually -20 db or less. The directivity of this coupler need not be high since for a fixed load and frequency, any error introduced in source power measurements by low directivity may be calibrated out.

In monitoring a load, a coupler will give an indication of how well the load is matched to the source. The coupling required for this coupler is a function of the sensitivity desired at the detector output. However, high directivity is required to measure small reflections. With a perfectly matched load (VSWR equal one), there would be no reflected voltage; therefore, the output voltage E_4 of

figure (2) should be zero since E_4 is proportional to E_{ref}. If E_4 is zero, then from equation (2) of figure (2), the directivity, D, is equal to infinity. This is perfect directivity and it means that none of the voltage of the main guide wave incident at terminal 1 travels in the backward direction in the auxiliary guide. With finite hole sizes for coupling elements, this is impossible even at a single frequency. However, directivities high enough to measure practical load VSWRs can be attained. For example, if it is desirable to measure the VSWR of a load down to 1.05, the directivity must be high enough not to introduce error signals which would be of the same order of magnitude as the reflection to be measured. A directivity of 32.2 db would introduce an error of equal magnitude as the reflection of a 1.05 load. If an attempt were made to measure a 1.05 load with a coupler having only 32.2 db directivity, by mechanically positioning the load, the magnitude of the voltage across the backward arm, E_4, would range from zero to twice the correct voltage. This variation is the result of the phase difference between the two equal magnitude voltages concerned. Therefore, in order to reduce the directivity error voltage to one-fifth of the reflected voltage of a 1.05 load, a directivity of 46 db is required.

If a single-ended directional coupler is set up to monitor reflected voltages, the reflected indication can be used to tune the load to a minimum reflection. However, if it is desired to read the coefficient of reflection without reversing the coupler, a bi-directional coupler must be used. This is the usage which fostered this study and the design of the coupler described later.

Directional couplers have also been used to introduce a signal to test receiver sensitivity. Also couplers have application as mixers.

4. Comparison with Slotted Lines and Hybrids

Load impedances can be measured either by measuring the reflection coefficient or the VSWR of a load. A bi-directional coupler measures direct, while a slotted line measures VSWR only after moving the output probe to two separate positions. The accuracies of the two are comparable. Good slotted lines have accuracies of _2%. This compares with a directivity of 40 db. Carefully designed couplers can do even better than this, but it seems the slotted line has reached its ultimate accuracy because of the discontinuity introduced by any probe. However, the slotted line can measure phase and magnitude while a coupler measures only magnitude.

When measuring low reflections, measuring with a coupler is more accurate than measuring VSWR by a slotted line. If higher reflections are to be measured, the use of a slotted line will give more accurate results.

A -3db coupler has the same division of power between main and auxiliary guides as a hybrid magic tee. Low reflections can be measured with the same accuracy with either the tee or the coupler, since each has approximately the same degree of isolation between arms. A small hole coupler, however, has the very distinct advantage of having a VSWR of 1.05 or less across the guide frequency band, whereas the tee is very frequency sensitive.

CHAPTER II

DESIGN CONSIDERATIONS

1. General

The specifications for a directional coupler of tight coupling and high directivity across a frequency band are difficult to meet. The tight coupling requires relatively large coupling apertures; but the larger the apertures the greater the interaction between coupling elements and the lower the directivity. Thus, these specifications are incompatible in this respect. However, both coupling and directivity increase with the number of coupling apertures, all other variables held fixed. It then becomes apparent that the best way to meet these specifications is (1) to use coupling apertures as large as possible without interfering with directivity, and then (2) to use as many coupling apertures as necessary to meet the required coupling and directivity. This approach will make the length of the coupler a minimum for any given specifications.

Although there are other designs* which can be used to obtain tight coupling, the so called multi-path directional couplers furnish the best possibility of satisfying both tight coupling and high directivity. In this type coupler there are several coupling elements along the guide length; and, therefore, there are many paths for the waves to travel. The directivity and coupling are achieved by wave interference, constructive for the forward wave and destructive for the

---

*For example, near-resonant slot couplers and branch guide couplers.

backward wave. The destructive interference is caused by phase difference due to path difference.

These multipath couplers are readily compared with antenna arrays. The voltage coefficient of directional couplers is computed in the same manner as the current feed of antenna arrays. Reference will be made to this comparison later.

First let us consider a two element coupler, which is the simplest form of multipath coupler. Its directivity is a result of (1) the quarter guide wave length spacing ($\lambda_g/4$) of coupling elements, and (2) the inherent directivity of a single hole as explained by Bethe.[1] The first of these is the greatest source of directivity and can be most easily explained by reference to figure (3). A voltage wave is transferred from the main to the auxiliary guide by each coupling element, which can be considered as a secondary source. Waves are emitted in all directions but wave motion is supported only along the guide in the TE_{10} mode. This means that each coupling element source transmits voltage waves in two directions. E_{B1} of figure (3) represents the voltage of the backward traveling wave (moving to the left) coupled through coupling element 1. E_{F1} represents the voltage of the forward traveling wave (moving to the right) coupled through coupling element 2. E_{F1} and E_{F2} travel the same path length and will reinforce to give a signal output at terminal 3 equal to E_{F1} plus E_{F2}. E_{B2} will be in phase opposition to E_{B1} since it has traveled one-half guide wave length further than E_{B1}. Therefore, the output at terminal 4 will be proportional to the difference of

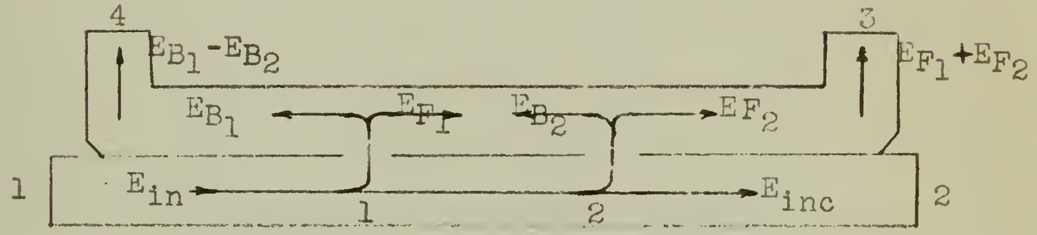

DIRECTIVITY OF A BIDIRECTIONAL COUPLER

FIGURE (3)

E_{B1} and E_{B2} if all terminations are perfectly matched. If the coupling elements or holes are of equal size E_{B1} equals E_{B2}. Furthermore, if they are infinitessimally small the path difference between E_{B1} and E_{B2} is exactly $\lambda g/2$, and no backward wave exists. Therefore, two practical limitations on perfect directivity at one given frequency (corresponding to λ_g), are hole size and longitudinal hole spacing. The problem is increasingly complex with the requirement of high directivity across a 20% bandwidth.

Several means of attaining tight coupling and high directivity over a broad band by use of multipath directional couplers will now be discussed in order to determine the design criteria of not only aperture* shape and size, but also aperture location.

2. Coupling

Coupling can be obtained in many ways through variously sized and shaped apertures. The apertures may be placed in either the small or the large dimension of the guide; and they may be located in various positions transversely and longitudinally along the guide and with respect to each other. Each of these dimensions mentioned are very critical and must be accurately computed and machined.

The first limitation placed on coupling elements is physical. Obviously they can be no larger than the dimensions of the guide. Also the size must be limited in order to make the small hole theory[1] valid.

*Coupling apertures are an obvious choice over probes and loops since the physical placement of the latter presents a problem.

The small hole theory will be discussed extensively in Chapter III. Working with small x-band wave guide, which supports frequencies from 8.2 to 12.4 KMC/sec, it has been shown[2] that the small hole theory was reasonably accurate up to hole diameters of .350 inches.

Miller and Mumford[3] achieved tight coupling up to complete transmission into the auxiliary guide by means of a long slot. Use was made of the 90° phase delay experienced when coupling from the main to the auxiliary guide, along with a second 90° phase delay resulting from coupling from the auxiliary to the main guide at the next aperture. The severe reflections normally encountered in slot couplers were avoided by placing wires transversely across the slot. These served to suppress the higher modes. Figure (4) illustrates this type coupling. This in effect divided the slot into several apertures. The small guide dimension was used for coupling. Both theoretical and experimental results show this type coupling to be frequency sensitive.

A second coupling theory using the binomial array type coupler was first introduced by Harrison[4] and later used by Mumford.[5] Each successive hole of a binomial coupler couples a voltage which is proportional to the coefficients of the terms of the binomial expansion to the 2N-1 power where 2N is the total number of elements. This array must use holes which are small enough to make the small hole theory valid in order to predict its performance. However, either face of the guide may be used for the coupling. If the large is used, the coupling across the band will be reasonably flat since

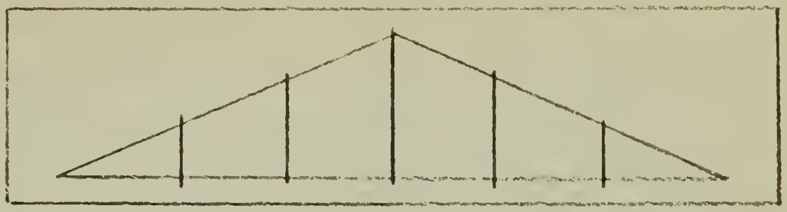

Miller-Mumford

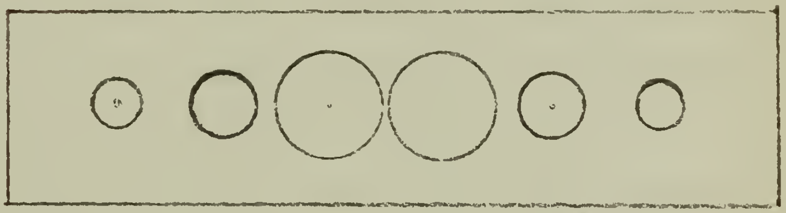

Binomial

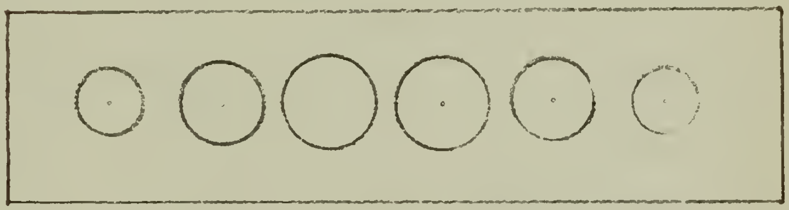

Tchebyscheff

COUPLING ELEMENT TAPER

FIGURE (4)

the frequency dependent part of the coupled voltage as shown later in equation (16), Chapter III is $(\frac{\lambda_g}{2a} + \frac{2a}{\lambda_g})$. The source of this term will be shown in the next chapter.

A third approach to obtaining the tight coupling required involves the use of Dolph's[6] antenna theory. It is similar to the binomial array coupler except that the voltage coefficients are made proportional to the normalized coefficients of the Tchebyscheff polynomial of order (2N-1) where 2N is the total number of elements. This multi-element array may be coupled on either face of the guide. The size of the holes will be limited not only by the physical dimensions but also by the small hole theory.

It was decided that the optimum shape of the apertures of either the binomial or the Tchebyscheff type couplers was round since this could be more easily machined than other odd shapes and still maintain tolerances. A double row of small coupling holes, would double the voltage coupling capability, i.e., increase voltage coupling by 6 db. Since the holes must be small to make the small hole theory valid and since the broad dimension will be used for coupling, this does not place too stringent physical limitations on the hole diameters. For small x-band, the internal guide dimensions are 0.9X0.4". For a doubled row of coupling holes, therefore, the largest possible radius of a coupling hole is .225", or a diameter of .450". Since hole sizes must be limited to less than .350" in order to apply the small hole theory in the small x-band region, the above mentioned physical limitation is not significant.

3. Directivity

The most obvious and universally used method of obtaining broadband directivity is that of varying the size of the coupling elements. This is known as taper. Figure (4) illustrates the methods of tapering used in the three previously discussed couplers. Also directivity increases directly with an increase in coupling elements. The limitation to this is the total practical length of a coupler.

Miller and Mumford point out that the backward wave in a coupler is related to the shape of the coupling slot by the Fourier transform.

$$I_b = F\int_{-L/2}^{+L/2} \varphi(z)\, e^{-j(4\pi/\lambda g) z}\, dz \qquad (2)$$

and $$I_f = F\int_{-L/2}^{+L/2} \varphi(z)\, dz \qquad (3)$$

L is total length of coupling slot

z is the longitudinal dimension of the guide

φ (z) is the shape of the coupling function

b is the small dimension of the guide

If the coupling were uniform over the interval of coupling, L, i.e., φ (z) equals one as shown in figure (5), then the directivity is given as

$$D = \frac{I_f}{I_b} = \frac{F\int_{-L/2}^{+L/2} (1)\, dz}{F\int_{-L/2}^{+L/2} (1)\, e^{-j(4\pi/\lambda g) z}\, dz} \qquad (4)$$

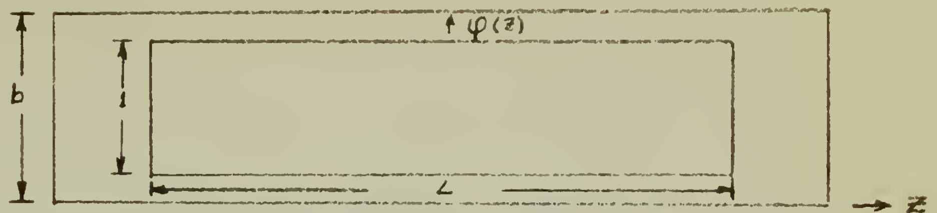

CONSTANT COUPLING PLATE BY MILLER-MUMFORD

FIGURE(5)

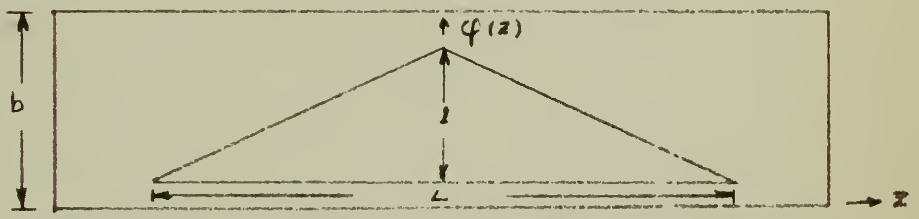

TAPERED COUPLING PLATE BY MILLER-MUMFORD

FIGURE(6)

Integrating and substituting the identity $\sin x = \frac{e^{jx} - e^{-jx}}{2j}$

$$D = \frac{L}{\frac{\sin(2\pi L/\lambda_g)}{2\pi/\lambda_g}} = \frac{2\pi L/\lambda_g}{\sin(2\pi L/\lambda_g)} \qquad (5)$$

Plotting directivity as a function of L/λ_g, it was found that high theoretical directivities were attained after a length, L, of 2 to 3 wave-lengths.

When the coupling function (z) was tapered as shown in figure (6), higher directivities for a given length, L, were attained when compared with the above constant coupling function. Actual measurements[3] of directivity made were found to be in close accord with this theory. However, this theory is presented with directivity as the primary object, and the coupling was loose and not easily determined theoretically in addition to being frequency sensitive. Coupling the large dimension with this tapered slot would eliminate the frequency sensitivity objection. However, it is felt that this interruption of the E-field would give results which could not be predicted by the small hole theory. Nevertheless, this is a practical approach and will undoubtedly be successfully applied in the future. Time did not permit a deeper investigation of its possibilities.

The binomial array is capable of giving very high directivity if enough holes are used. The theoretical directivity versus frequency plot of this type coupler will result in infinite directivity at the design frequency, f_o. The directivity is still high very close to f_o but becomes increasingly worse the farther it is removed.

With a Tchebyscheff array[6], the directivity is theoretically infinite at several frequencies across the suppression band. This occurs with an oscillatory action which is a function of the order of the Tchebyscheff polynomial. Possibly it is easier to explain the directivity when working with an antenna pattern as illustrated. by Dolph. A zero side lobe radiation can be compared with a zero backward wave (infinite directivity). In the terminology of a directional coupler, a coupler which has 2N coupling elements which couple voltage in proportion to the coefficients of a Tchebyscheff polynomial of order 2N-1, will have a computed backward wave which will oscillate about zero with a ripple of constant magnitude across the designed suppression band. Thus a Tchebyscheff array has a maximum error which is independent of frequency while the backward voltage of a binomial array is a function of frequency.

CHAPTER III

THEORETICAL DESIGN

After weighing the above-mentioned considerations of coupler design, it was decided to attempt to design and build a Tchebyscheff small hole type coupler with -3db coupling and 40 db directivity across the frequency band of 8 to 10 kmc/sec. The large dimension was used for coupling in order to take advantage of the 6 db gain in coupling two rows of small holes, as well as obtaining relatively frequency insensitive coupling. In addition advantage can be made of the inherent directivity which will be discussed later.

Bethe's[1] small hole theory is valid if the following limitations are imposed:

(1) the coupling hole is much less than λ_g

(2) the holes are in an infinitely thin wall

(3) that the holes are far from corners, and

(4) that measurements are made far enough from the holes that the higher order modes excited there have been damped out.

Assuming that these limitations are satisfied, we can make use of the following expressions:

$$E_3 = \sum_{n=1}^{2N} A_n \tag{6}$$

$$E_4 = \sum_{n=1}^{2N} B_n \cos(2n-1)\beta z \tag{7}$$

or due to symmetry

$$E_3 = 2\sum_{n=1}^{N} A_n \tag{8}$$

$$E_4 = 2\sum_{n=1}^{N} B_n \cos(2n-1)\beta z \tag{9}$$

where E_3 and E_4 are the outputs as shown in figure (2)

2N is number of longitudinally distinct coupling holes

A_n is the forward coefficient of coupling for coupling hole "n"

B_n is the backward coefficient of coupling for coupling hole "n"

n 1,2,3,4,.....N

$\beta = 2\pi/\lambda_g$

z is the longitudinal coordinate of the guide

Equation (8) merely says that the voltage coupled in the forward direction is equal to the sum of all the voltages coupled by the individual apertures. Equation (9) states the same thing for the backward voltage but has the directional factor introduced by virtue of path difference.

Now considering the Tchebyscheff polynomials as defined by[7]

$$T_m(x) = \cos(m\cos^{-1}x) \qquad -1 < x < +1 \tag{10}$$

$$T_m(x) = \cosh(m\cosh^{-1}x) \qquad |x| > 1 \tag{11}$$

If x equal to $\cos\beta z$ is substituted for the argument of equation (10), it becomes

$$T_m(\cos\beta z) = \cos m\beta z \quad \text{for} \quad \pi > \beta z > 0 \tag{12}$$

with $m = (2n-1)$, equation (12) is in the form of equation (9) since the expansion of equation (12) contains only terms in $\cos(2n-1)\beta z$ and the terms end with $n = N$. Therefore, if the backward coefficients

of coupling, B_n, can be made proportional to the corresponding coefficients of the Tchebyscheff polynomial of order 2N-1, the theoretical directivity will have a suppression band of equal-ripple magnitude. These coefficients are developed in Appendix (B).

Now a design parameter, z_0[6], which determines the width of the suppression band, must be established. The value of 1500:1 for a ratio of forward to backward waves was chosen. This gives a D=63.5 db which was considered to be sufficient overdesign. Equation (13) determines z_0 as follows:

$$z_0 = \frac{1}{2}\left[(g + \sqrt{g^2-1})^{1/m} + (g - \sqrt{g^2-1})^{1/m} \right] \qquad (13)$$

In this equation, m is equal to 2N-1; the value of 2N was established at 10 as a good compromise to limit hole size and still attain -3 db coupling. In addition the higher order Tchebyscheffs become difficult to manipulate mathmatically. Thus for g=1500 and m=9, equation (13) was solved and z_0 was found to be 1.42.

With this value of z_0, the coefficients of a Tchebyscheff polynomial of order 9 were solved for. See Appendix (B). Making the coefficients of coupling proportional to the Tchebyscheff coefficients, and solving for hole size (this method to be shown later) resulted in the fact that for -3db coupling the holes would overlap. However, this overlap result produced the idea of superimposition[2,4] of coupling coefficients to attain a reasonable size hole with the degree of coupling required. The result was the superimposition of four ten element arrays which resulted in a 22 element superimposed

Tchebyscheff type array. See Appendix (B) and figure (7).

From Appendix (B), the total of all the Tchebyscheff coefficients, T_t, for the 44 coupling holes (two rows of 22) is 476.16. The total coupling ratio, A_t, for -3 db coupling is

$$Cdb = 20 \log A_t \qquad A_t = .708 \tag{14}$$

The Tchebyscheff coefficients for the individual holes, T_n, are tabulated in Appendix (B). Therefore, the forward coefficient of coupling for each individual hole, A_n, can be determined by solving the following simple ratio:

$$2x \frac{A_n}{A_t} = \frac{T_n}{T_t} \tag{15}$$

It may be noted that n needs to run only from 1 to 11 since the array is longitudinally symmetrical, and the pairs of holes located in the same transverse position are of the same size, as shown in figure (8).

From the small hole theory^1, the following expressions are for the forward voltage coefficient and the backward voltage coefficient, respectively, of one individual hole; n.

$$A_n^* = j\frac{2\pi r_n^3}{3a^2 b}\left\{\alpha_E\left(\frac{2a}{\lambda_g} + \frac{\lambda_g}{2a}\right)\sin^2\frac{\pi x_1}{a} - 2\alpha_H\left(\frac{2a}{\lambda_g}\right)\sin^2\frac{\pi x_1}{a} - 2\alpha_H\left(\frac{\lambda_g}{2a}\right)\cos^2\frac{\pi x_1}{a}\right\} \tag{16}$$

$$B^* = j\frac{2\pi r_n^3}{3a^2 b}\left\{\alpha_E\left(\frac{2a}{\lambda_g} + \frac{\lambda_g}{2a}\right)\sin^2\frac{\pi x_1}{a} + 2\alpha_H\left(\frac{2a}{\lambda_g}\right)\sin^2\frac{\pi x_1}{a} - 2\alpha_H\left(\frac{\lambda_g}{2a}\right)\cos^2\frac{\pi x_1}{a}\right\} \tag{17}$$

---

*These are developed in Appendix A.

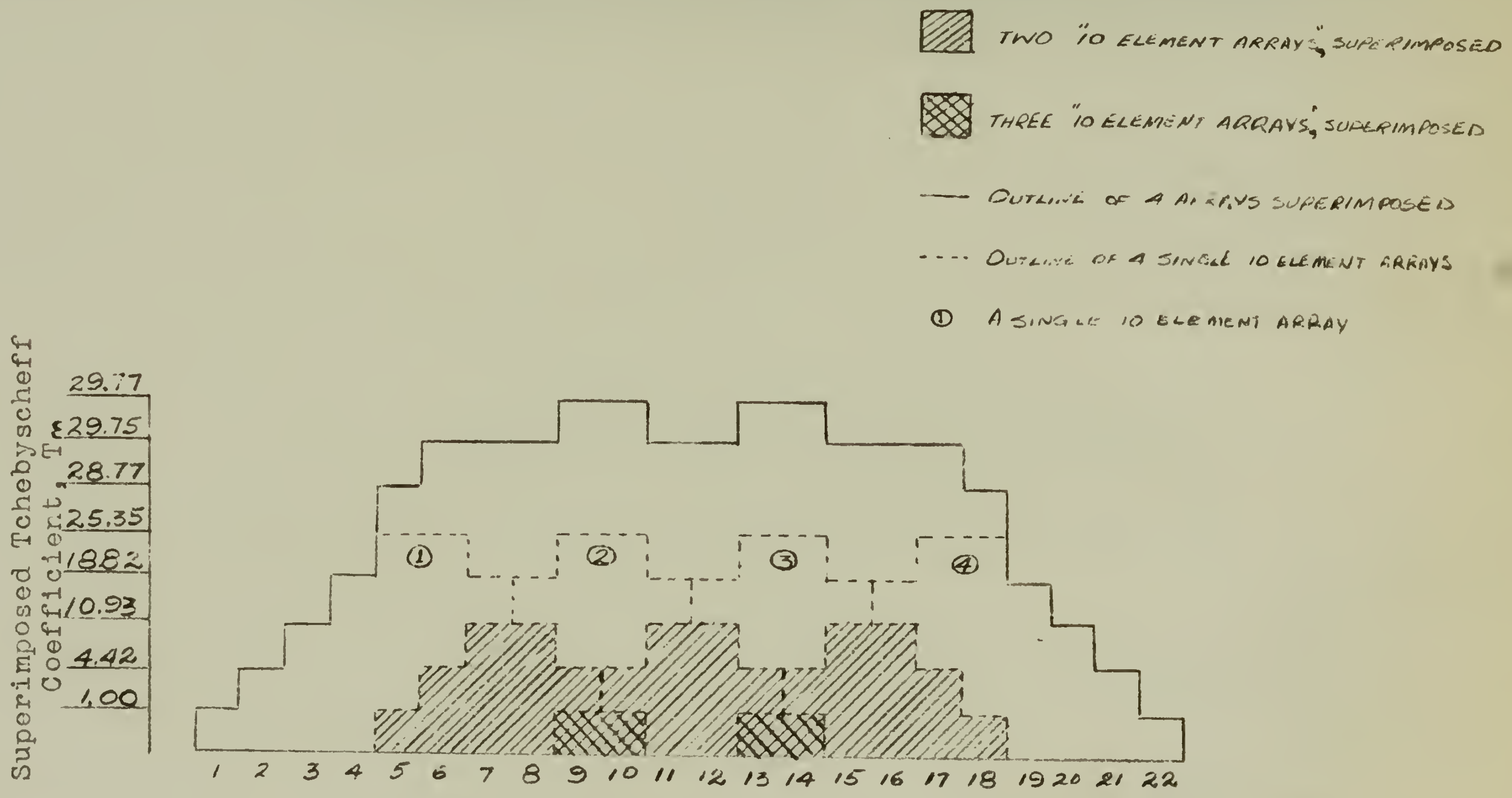

SUPERIMPOSED TCHEBYSCHEFF COEFFICIENTS BY BARNETT

FIGURE (7)

COUPLING PLATE, FINAL DESIGN FOR 3 DB COUPLING
40 DB DIRECTIVITY

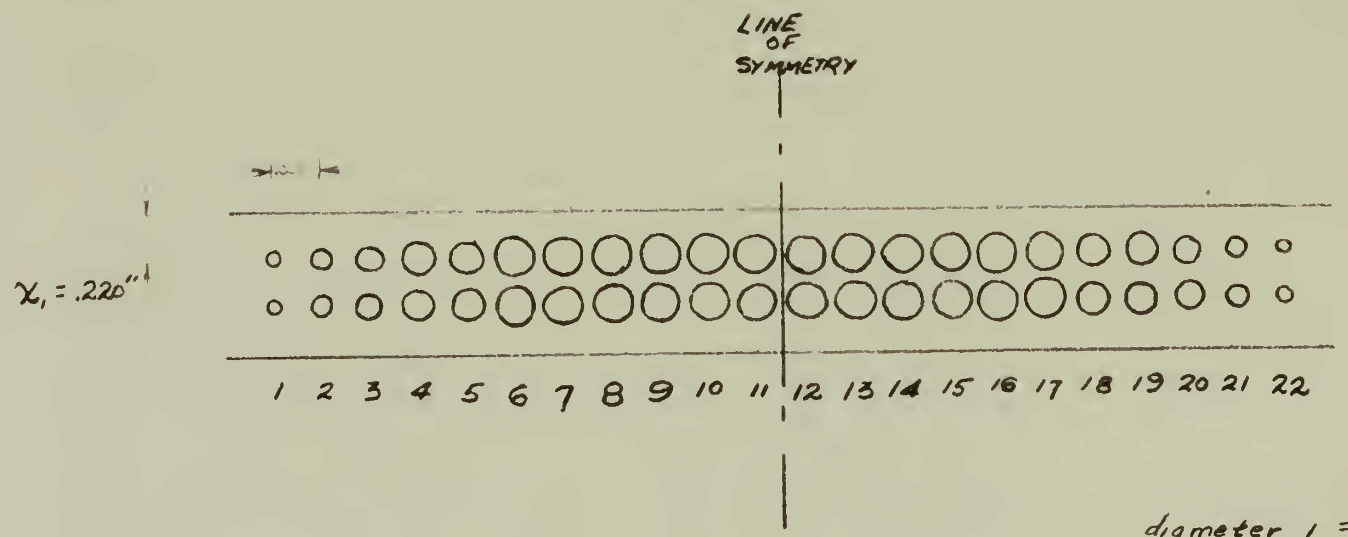

	THEORETICAL	MEASURED
diameter 1 =	.121	.121
" 2 =	.184	.184
" 3 =	.240	.238(1)
" 4 =	.282	.281(1)
" 5 =	.308	.3045(2)
" 6 =	.320	.321(1)
" 7-11 =	.324	.323(20)

FIGURE (8)

where	a	large inner dimension of the guide
	b	small inner dimension of the guide
	r	radius of the coupling hole
	λ_g	guide wave-length
	x_1	distance from side of guide to the center of the coupling hole
	z_1	spacing center to center between holes
	α_ε	electric field attenuation factor due to guide thickness
		See figure (9)

The three terms in the brackets arise from the electric field, the transverse component of the magnetic field, and the longitudinal component of the magnetic field, respectively. These are complex relations which are very unwieldy unless some simplifying assumptions are made. If the variables of equation (16) can be separated by legitimate approximations a coupling design may be established.

The variables and are attenuation factors due to the finite wall thickness in which the holes are drilled. By use of these factors, limitation (2) on page 16 is no longer a restriction. These holes are considered as circular wave guides below cutoff. The electric field term from equation (16) sets up a TM_{01} mode, while the magnetic field corresponds to the TE_{11} mode. Since the TM_{01} mode is farther below cutoff, it is attenuated more than the TE_{11} mode. Therefore, the coefficient of attenuation for the

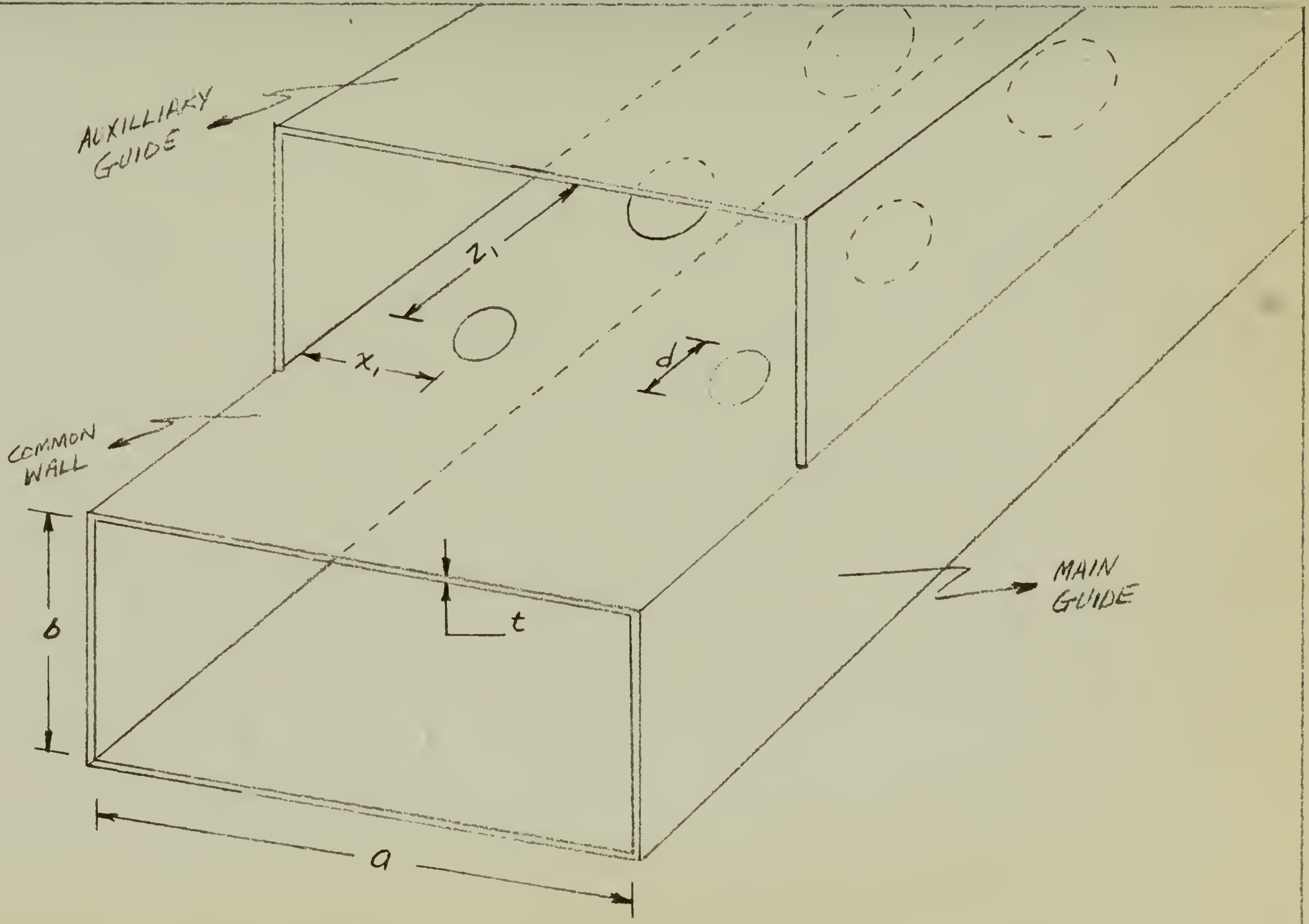

FIGURE (9)

magnetic field α_H is larger than the coefficient α_E.

$$\alpha_E(\rho, \lambda) = e^{-2.405\, t/r\, [1 - (\frac{2.613\, r}{\lambda})^2]^{1/2}} \tag{18}$$

$$\alpha_H(\rho, \lambda) = e^{-1.841\, t/r\, [1 - (\frac{3.412\, r}{\lambda})^2]^{1/2}} \tag{19}$$

where ρ is a geometry factor which varies with the thickness, t, of the common wall and the radius, r, of the hole. λ is free space wavelength. (See figure (9).

The first approximation made in the small hole theory, equations (16) and (17) follows. Expanding the radical in the exponent of α_E by the binomial theorem expansion, the second order and higher terms may be thrown out. Therefore equations (18) and (19) become functions of ρ alone; and further, upon fixing a value for the common wall thickness, α_E and α_H become functions of the radius alone. Then equations (18) and (19) become

$$\alpha_E(\rho) = e^{-2.405\, t/r} \tag{20}$$

$$\alpha_H(\rho) = e^{-1.841\, t/r} \tag{21}$$

This first order approximation is a help in simplification; however, the variables r and λ_g are still not separable in equation (16). Thus a second approximation is introduced. Since the α_H term appears in two terms and α_E appears in one term of equation (16) a weighted attenuation factor will give a closer approximation than the use of the predominant α_H.

Therefore, let equations (20) and (21) become

$$\alpha_E(\rho) = \alpha_H(\rho) = \alpha_{EH}(\rho) = e^{-2.029t/r} \qquad (22)$$

Now the λ_g terms and the r terms of equation (16) may be separated. The forward coupling coefficient can now be written in the followinf forms:

$$A(\rho,\lambda_g) = j\frac{2\pi\cdot r^3}{3a^2b}\alpha_{EH}\left\{\left(\frac{2a}{\lambda_g}+\frac{\lambda_g}{2a}\right)\sin^2\frac{\pi x_1}{a} - \left(\frac{2a}{\lambda_g}\right)2\cdot\sin^2\frac{\pi x_1}{a} - \left(\frac{\lambda_g}{2a}\right)2\cdot\cos^2\frac{\pi x_1}{a}\right\} \qquad (23)$$

$$|A(\rho,\lambda_g)| = |K(\rho)|\cdot|F_A(\lambda_g)| \qquad (24)$$

where

$$|F_A(\lambda_g)| = \left\{\left(\frac{2a}{\lambda_g}+\frac{\lambda_g}{2a}\right)\sin^2\frac{\pi x_1}{a} - 2\left(\frac{2a}{\lambda_g}\right)\sin^2\frac{\pi x_1}{a} - 2\left(\frac{\lambda_g}{2a}\right)\cos^2\frac{\pi x_1}{a}\right\} \qquad (25)$$

$$|K(\rho)| = \frac{2\pi r^3}{3a^2b}\alpha_{EH}(\rho) = \frac{2\pi r^3}{3a^2b}e^{-2.029t/r} \qquad (26)$$

The value of x_1 was established by plotting $|F_A(\lambda_g)|$ vs. x_1 at the two extermities of λ_g for small x-band guide. (Figure (10)) This will give the least deviation of coupling across the band. The intersection of these two curves established x_1 at 0.22 inches.

The design value of λ_g was established from a plot of $|F_A(\lambda_g)|$ vs. λ_g. A horizontal line was drawn at the mean value of $|F_A(\lambda_g)|$. In the final plot of coupling this will coincide with -3 db. This mean existed for two separate values of λ_g. The smaller λ_g was chosen in order to make the overall length of the coupler less. λ_g design was

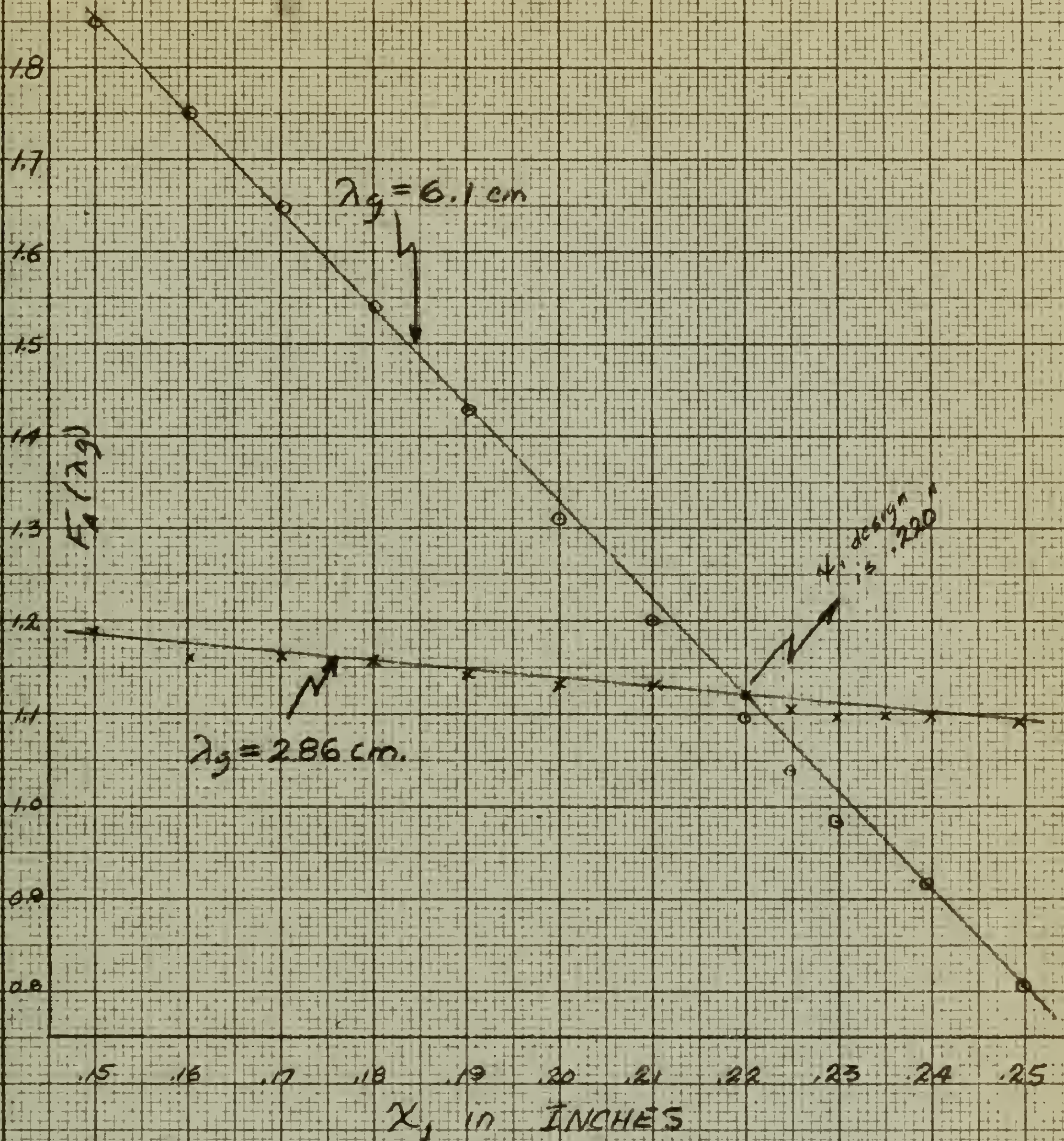

$F_A(\lambda g)$ vs. X_1

FIGURE (10)

established in this manner at 3.24 cm (z_1 = .319"). See design figure (11). It will be shown later that z_1 had to be increased. It was finally established at .350".

The value of equation (25) at the design frequency ($\lambda_g/4 = .350$) is a constant, i.e.,

$$|F_A(\lambda_g)|_{1.40''} = 1.05 \tag{27}$$

From equation (24)

$$|A(\rho)|_{\lambda_g = 1.40''} = 1.05\ K(\rho) = 1.05 \times \frac{2\pi r^3}{3a^2 b} e^{-2.029\,t/r} \tag{28}$$

For t = .025", a = .9", and b = .4", equation (28) becomes

$$|A(r)_n| = 6.79\ r_n^3\, e^{-.046/r_n} \tag{29}$$

By inspection of equation (17), it is seen that

$$|B(\rho,\lambda_g)| = |K(\rho)| \cdot |F_B(\lambda_g)| \tag{30}$$

where

$$|F_B(\lambda_g)| = \left\{ \left(\frac{2a}{\lambda_g} + \frac{\lambda_g}{2a} \right) \sin^2 \frac{\pi x_1}{a} + 2\left(\frac{2a}{\lambda_g} \right) \sin^2 \frac{\pi x_1}{a} - 2\left(\frac{\lambda_g}{2a} \right) \cos^2 \frac{\pi x_1}{a} \right\} \tag{31}$$

$$|F_B(1.40'')| = 1.44 \tag{32}$$

$$|B(r)_n| = 9.30\ r_n^3\, e^{-.046/r_n} \tag{33}$$

Equations (29) and (33) are identical except for a constant coefficient. In order to get the correct coupling, the $A(r)_n$'s

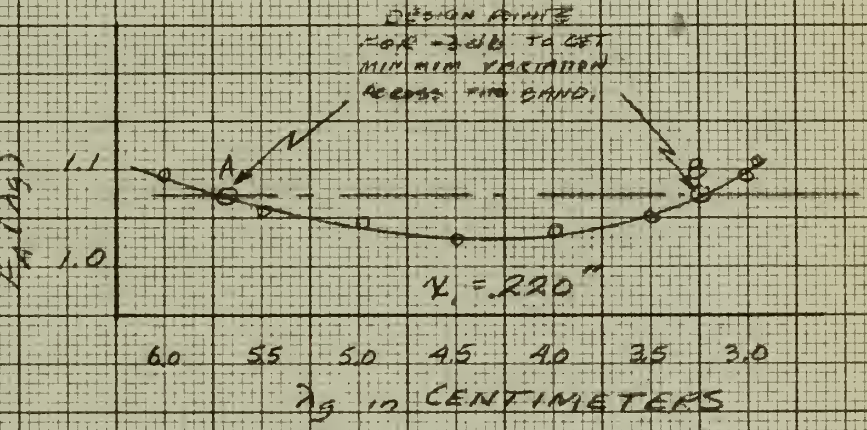

$F_A(\lambda g)$ vs. λg

FIGURE (11)

should be proportional to the Tchebyscheff coefficients. On the other hand if the directivity is to be of equal ripple magnitude, the $B(r)_n$'s should be set proportional to the Tchebyscheff coefficients. The coupling should be within less than 1 db of -3 db, whereas the directivity can be anything as long as it is greater than 40 db. Therefore, the $A(r)_n$'s were used as the design coefficients.

The transcendental equation (29) was solved by assuming values of r and plotting $A(r)_n$ vs. r_n where n 1,2,3,.....11, which is the number of the particular hole considered. Taking the values of A_n solved for previously by equation (15), the diameter of a particular hole may be found, by entering the plot of equation (29). This is only approximate since it is only as good as the curve can be read. This must be checked by solving equation (29) with the approximate radius to find its agreement with the true A_n. This is repeated until the required accuracy of ± .001" is obtained for the radii. The final radii values of the 44 coupling holes are shown in figure (5). Note the largest hole size is d = .324". $\lambda_g/4_{des.}$ must be greater than this to avoid overlap. Mechanical limitations require at least .010" between the circumferences of the holes. This z_1 was established previously at .319" to give a minimum deviation of coupling. However, since it must be increased, it was arbitrarily set at .350".

Thus having established the following design parameters, the coupler is complete:

(1) small x-band guide

(2) hole sizes, r_n, n = 1,2,3,4,.......11.

(3) x_1, the transverse hole position

(4) z_1, the longitudinal hole position, which also establishes the design frequency,

See figure (5) for the final design.

CHAPTER IV

EXPERIMENTAL RESULTS

The above coupler was manufactured as shown in the photograph, figure (12). The specified tolerance for the diameters of holes was ±.001". Some of the holes were measured and found to be outside of this tolerance. The actual sizes are indicated in figure (8).

The experimental laboratory setup for testing this coupler is shown in the block diagram of figure (13). The measurement of coupling is straight forward. Coupling as defined in equation (8) was measured by the Hewlett-Packard 415A amplifier. A plot of coupling vs. frequency is shown in figure (14).

The directivity measurements require very exacting laboratory techniques due to the high voltage differentials measured. Referring to figure (15), note that the output mitre joint of terminal 3 has been left off. Terminal 2 and 3 are then terminated with sliding loads which are 1.05 or better across the band. By the following technique the effect of the load reflections can be eliminated. Let $\vec{E}_2'$ and $\vec{E}_3'$ be the reflected voltage vectors of their respective terminals.

$$\vec{E}_2' = E_2' e^{j\theta_2'} \tag{34}$$

$$\vec{E}_3' = E_3' e^{j\theta_3'} \tag{35}$$

Let $\vec{E}_4$ be the output voltage of terminal 4 and $\vec{E}_m$ be the portion

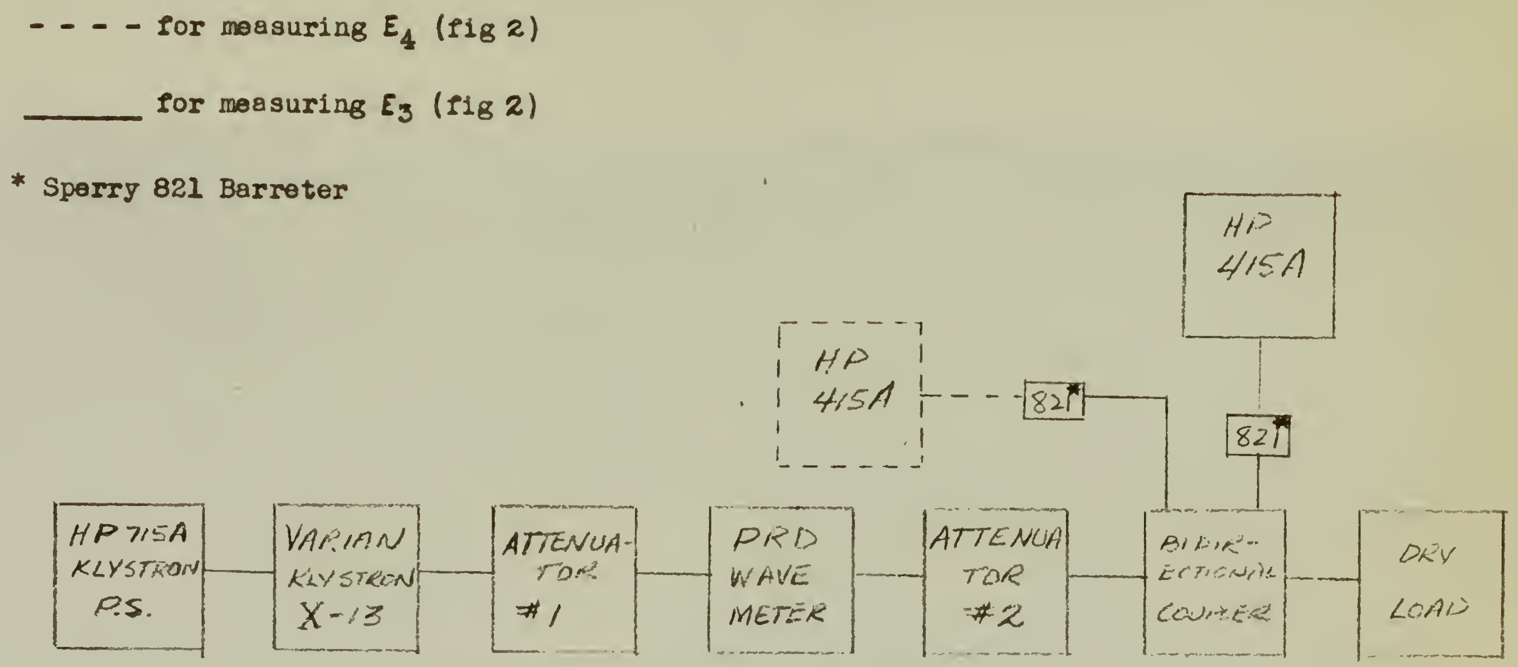

Laboratory Bench Setup for Measuring
Coupling and Directivity
of a Bi-directional Coupler

FIGURE (13)

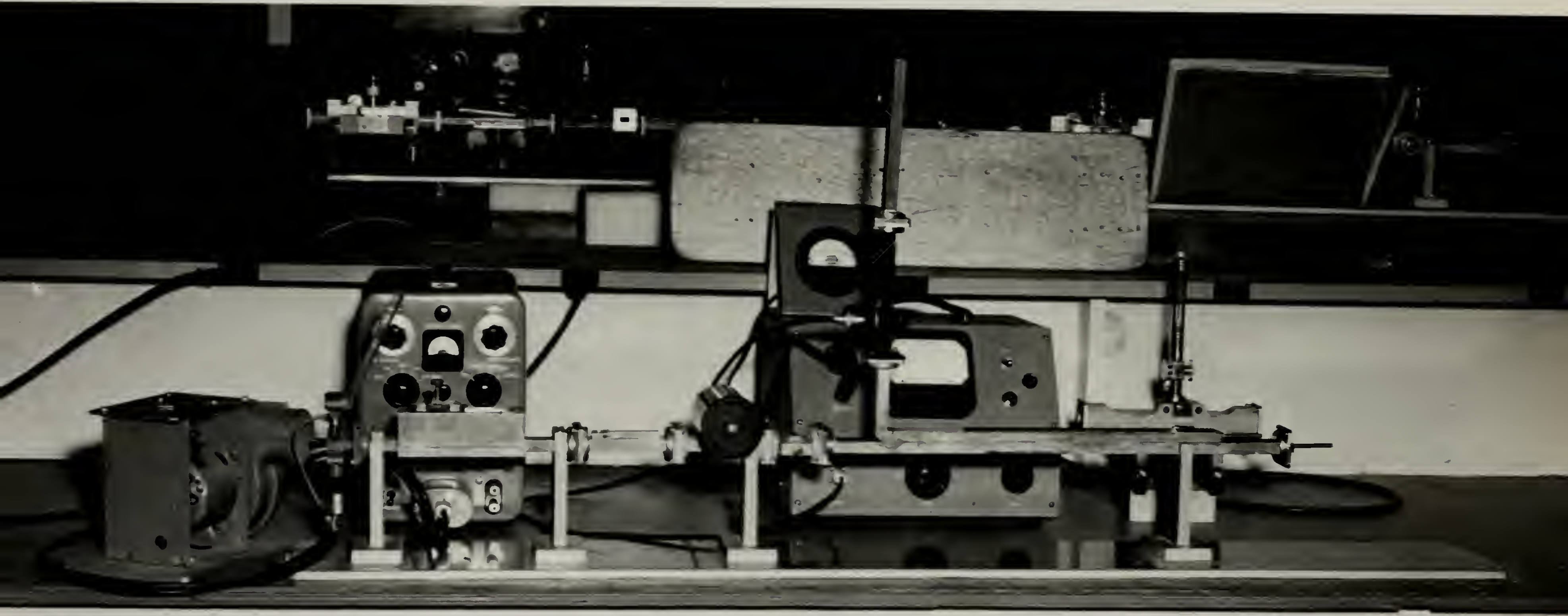

FIGURE (12)

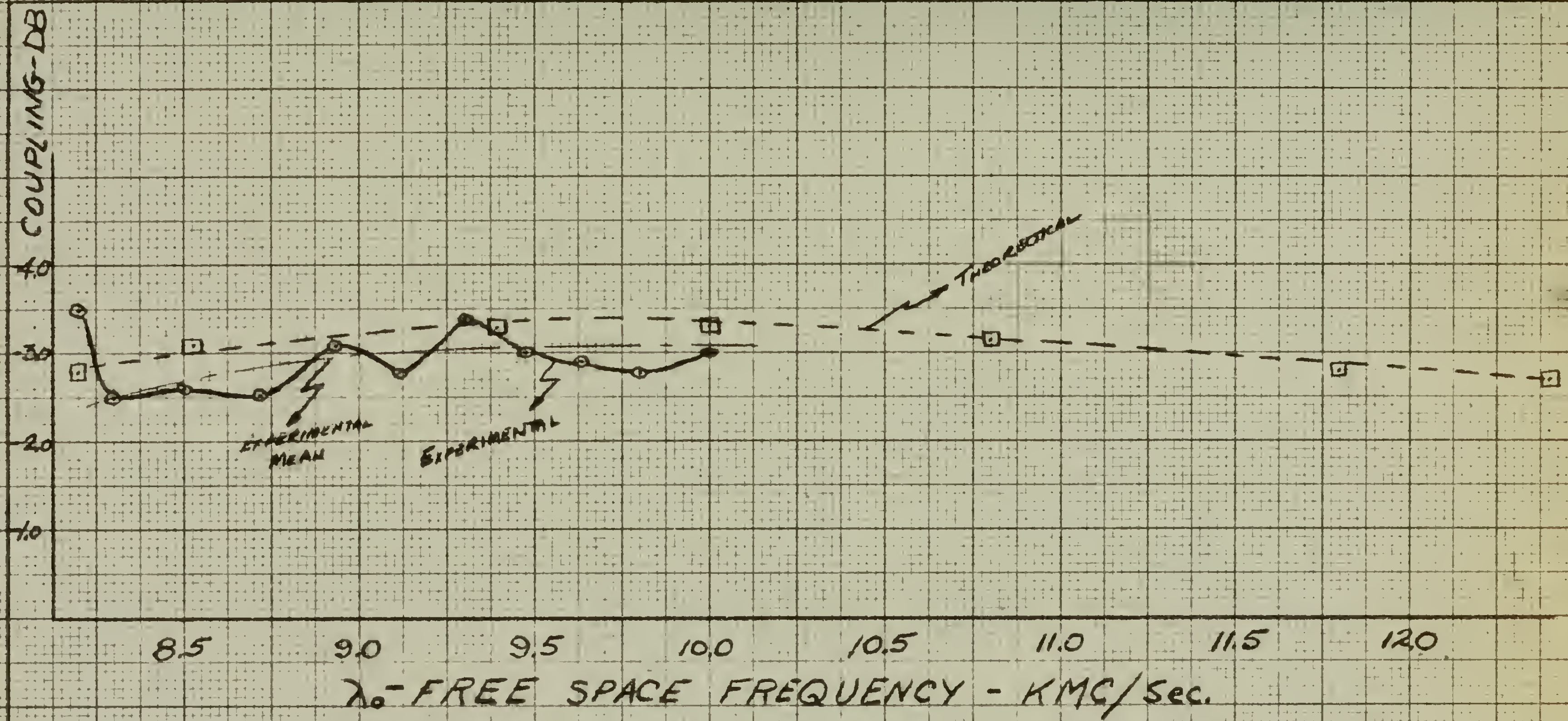

THEORETICAL AND ACTUAL COUPLING CURVES

FIGURE (14)

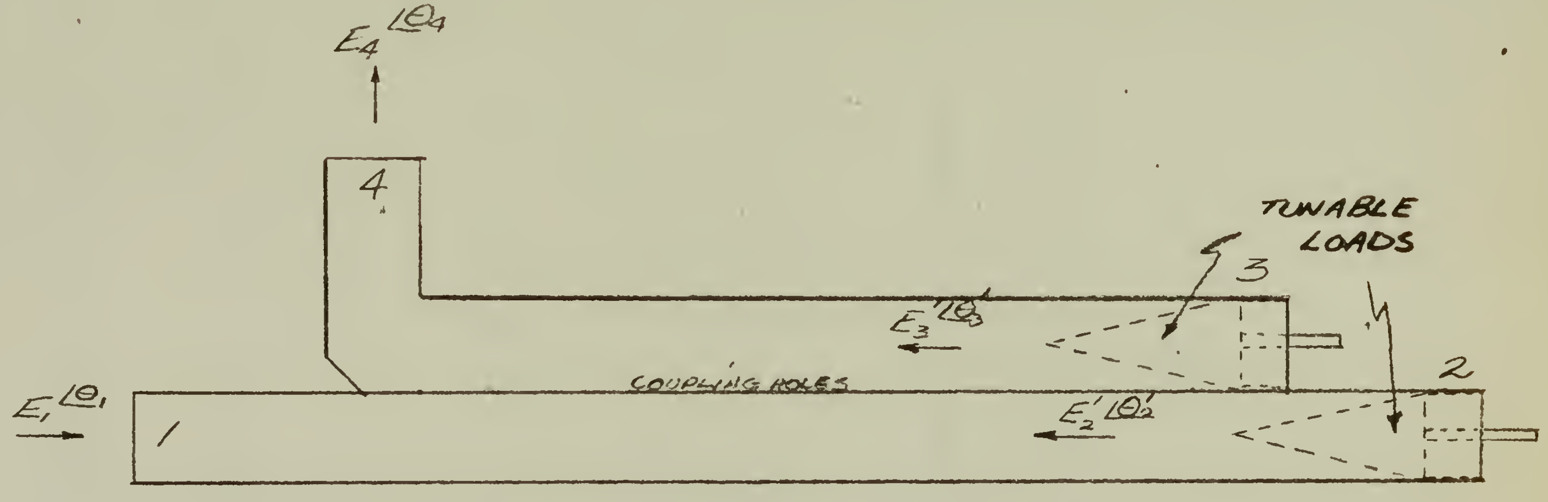

An Illustration of the Technique
Involved in Measuring High
Directivities

FIGURE (15)

of $\vec{E}_4$ which is due to imperfect directivity. $\vec{E}_m$ is the voltage for which we must solve.

$$\vec{E}_4 = E_4 e^{j\theta_4} \tag{36}$$

$$\vec{E}_m = E_m e^{j\theta_m} \tag{37}$$

then

$$\vec{E}_{4max} = \vec{E}_m + \vec{E}_3' + k_c^* \vec{E}_2' \tag{38}$$

If the sliding loads are carefully tuned for a maximum output signal at terminal 4, then all of the phase angles are equal and the vector magnitudes may be added directly.

$$E_{4max} = E_m + E_3' + k_c E_2' \tag{39}$$

Now tuning the two sliding loads for a minimum output reading at terminal 4, means that the phase of E_m is 180° out with the phase of E_3 and E_2. Thus

$$E_{4min} = E_m - (E_3' + k_c E_2') \tag{40}$$

Solving these equations gives

$$E_m = \frac{E_{4max} + E_{4min}}{2} \tag{41}$$

The coupler is then reversed and the voltage output of terminal three, E_3 is measured.

---

*A constant less than one due to coupling

The db difference between E_3 and E_m is the directivity, i.e.,

$$D = E_{3db} - E_{mdb} \tag{42}$$

A plot of this directivity vs. frequency is shown in figure (16).

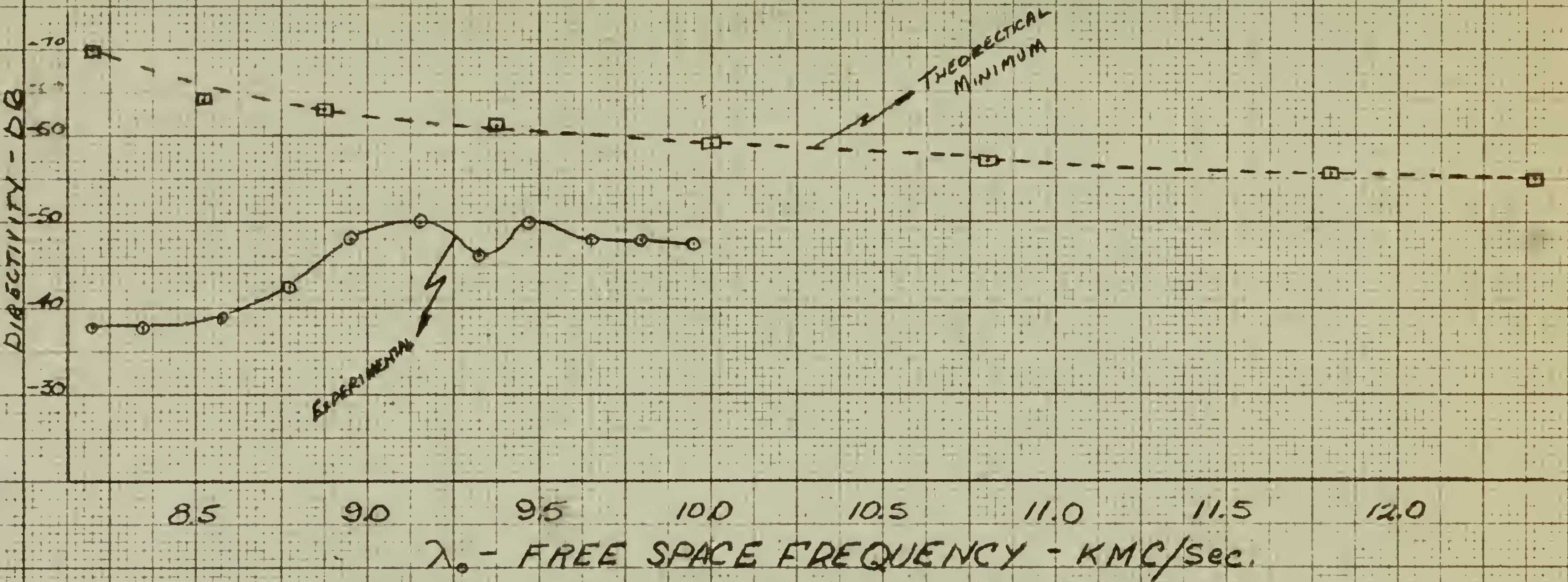

THEORETICAL AND ACTUAL DIRECTIVITY CURVES

FIGURE (16)

CHAPTER V

CONCLUSION

1. General

The experimental design of the bi-directional coupler has been compared with the theoretical curves, in figures (14) and (16). In general it is felt that the results have been very close to the theory. The experimental results show that the coupler has fallen slightly outside of specifications. However, it must be stated that this coupler was designed entirely theoretically. No benefit from laboratory experience was available prior to the ultimate design. It is felt that the deviations from the specifications can be justified and corrected in future models. An attempt will be made to evaluate these justifications.

2. Coupling

The theory predicted a range in coupling, as shown in figure (14) from -2.66 db at 8.2 kmc to a minimum of -3.31 db at 9.4 kmc. This gives a db difference of .65. The actual measured coupling ranged from -2.5 db at 8.3 kmc to -3.4 db at 9.25 kmc, or a db difference of 0.9. The actual coupling of -3.5 db at 8.26 kmc seems to be in error, so it will not be considered. The solid red line appears to be a realistic mean for the experimental coupling. This is an average error of about -0.4 db.

The following are possible contributions to this error:

(1) Mechanical tolerances of ±.001" were requested but not obtained for the critical coupling dimensions. Such tolerances can be held. Since the radii were under size in all cases out of tolerance, this would indicate that the experimental result would show less coupling than the theoretical. This is not the overall case.

(2) The first approximation introduced a first order error as can be seen by comparison of equations (19) and (21). If second order accuracy is used, the term $\left(1 - \frac{(3.412r)^2}{(\lambda)^2}\right)^{1/2}$ becomes $\left(1 - \frac{1}{2}\left(\frac{3.412r}{\lambda}\right)^2\right)$ instead of "1", by the first order theory. The greatest error this approximation can introduce occurs when r is maximum or .411 cm and λ is minimum or 2.42 cm. The coupling using the first order theory gave -2.38 db. Thus the first order approximation has the affect of encreasing coupling, which is the overall case.

(3) The second approximation indicated in (22) is a very good one. However, it introduces a small error which makes the actual coupling tighter than the theoretical.

(4) Laboratory technique can be a random contribution to coupling measurement errors. It is estimated that the laboratory measurements are accurate to ± 0.2 db.

(5) The larger the radius of the coupling holes with respect to a wave length, the less valid is the first order theory. The largest hole diameter of this coupler is .324". This is becoming an appreciable part of a free space wave length which for 9 kmc is

1.31". This is an error which aggravates the second error listed above.

In consideration of these error possibilities, it is possible to reconcile partially at least, the theoretical with the experimental.

3. Directivity

As shown in figure (16), the experimental directivity has a minimum of 37.8 db at 8.26 kmc. It is below specifications from 8.26 to 8.5 kmc. There are several contributing factors.

First the theoretical directivity will be inspected. From figure (2), it is seen that

$$D = 20 \log \left| \frac{E_3}{E_4} \right| \tag{43}$$

Substituting (6) and (7) in (43)

$$D = 20 \log \frac{\sum_{n=1}^{N} A_n}{\sum_{n=1}^{N} B_n \cos(2n-1)\beta z} \tag{44}$$

Now substituting (24) and (30) into (44)

$$D = 20 \log \frac{F_A(\lambda_g)}{F_B(\lambda_g)} + 20 \log \frac{\sum_{n=1}^{N} K(\rho)}{\sum_{n=1}^{N} K(\rho) \cos(2n-1)\beta z} \tag{45}$$

The first term of (45) is a type of directivity which is inherent with any single hole. It can be either positive or negative. It gives positive directivity at the low frequencies and negative directivity at the higher frequencies. This is opposite to the error existing in this coupler.

The second term is the source of equal-ripple magnitude of reverse wave radiation. However, this optimum directivity is affected by the wide variation of the inherent directivity. But this is not the only source causing directivity to fall off.

The interactions between the holes of this multi-hole coupler in the fundamental as well as higher modes is undoubtedly a source of error. The hole sizes as stated under "coupling" above are another serious limitation, as well as the mechanical tolerances attainable.

Probably, the largest contribution to this error was made by a design error. The λ_g design used was 3.56 cm which corresponds to a frequency of 10.7 kmc. This is obviously a very poor design frequency for obtaining directivity from 8 to 10 kmc. This accounts for the drop-off in directivity at the lower frequencies, which are getting near the limit of the suppression band as determined by z_0. A design of 4.25 would center this optimum directivity at about 9.0 kmc. This of course would lengthen the coupler considerably, but this should easily give 40 db directivity from 8 to 10 kmc.

This coupler is also a compromise in length. Greater coupling length will allow the use of more holes with a decrease in the size of the holes. This will increase both directivity and coupling accuracy.

Thus although it is very difficult to account for the results quantitatively, this qualitative discussion does give some justification to the resultant errors.

BIBLIOGRAPHY

1. Bethe, H. A. Lumped Constants for Small Irises Radiation Laboratory Report # 194, MIT, 24 March 1943.

Theory of Side Windows. Radiation Laboratory Report # 199, MIT, 4 April 1943.

Excitation of Cavities through Windows Radiation Laboratory Report # 202, 9 April 1943.

Theory of Diffraction by Small Holes, Physical Review, second series, Vol 66, Nos 7 and 8, Oct 1 and 15, pp 163-182.

Also pp 858-866 on Bethe Hole Theory of C.G. Montgomery's Techniques of Microwave Measurements, McGraw-Hill 1947, Radiation Laboratory Series # 11.

2. Barnett, E. F. of Hewlett-Packard Company, Palo Alto, California in unpublished paper.

3. Miller, S. E. and Mumford, W. W. Multi-Element Directional Couplers. Proc. of IRE Vol 40 No 9, September 1952.

4. Harrison, R. J. Design Considerations for Directional Couplers, Radiation Laboratory Report # 724, MIT 31 December 1945.

5. Mumford, W. W. Directional Couplers. Proc. of IRE, Vol 35, No 2, February 1947.

6. Dolph, C. L. A Current Distribution for Broadside Arrays which Optimize the Relationship between Beam Width and Side Lobe Level. Proc. of IRE, Vol 34, No 6, June 1946.

7. Jordan, E. C. Electromagnetic Waves and Radiating Systems. Prentice-Hall 1950, pp 440-445.

APPENDIX A

THE VOLTAGE COUPLING COEFFICIENTS FOR THE TE_{10} MODE AS DEVELOPED FROM BETHE'S SMALL HOLE THEORY

Bethe[1] describes the voltage coupled through a small aperture by three lumped constants, namely two magnetic polarizabilities, M_1 and M_2, and one electric polarizability, P. These constants determine the effect of any aperture on the wave guide. For simple shapes such as circles, ellipses, and slits, these polarizabilities have been calculated. Note that these constants are independent of the field. They depend only on the geometry of the aperture.

For the TE_{10} mode, Bethe's formula for the voltage coefficient for the forward wave is

$$A = \frac{j\pi}{\lambda_0 S}\left(P\, E_{y1} E_{y2} - M_1 H_{x1} H_{x2} - M_2 H_{z1} H_{z2}\right) e^{-j(\omega t - \beta z)} \qquad (46)$$

where λ_0 = free space wave-length

S = normalizing factor $\frac{2a^3bC^2}{\lambda_g \lambda_0}$

P = electric polarizability for a round hole = $2r^3/3$

M_1 = transverse magnetic polarizability for a round hole = $4r^3/3$

M_2 = longitudinal magnetic polarizability for a round hole = $4r^3/3$

E_{y1}, H_{x1}, H_{z1} - field components in the main guide

E_{y2}, H_{x2}, H_{z2} - field components in the auxiliary guide

$\beta = \frac{2\pi}{\lambda_g}$ λ_g is guide wave length

x is the principal axis in the direction of the large guide dimension, a

y is the principal axis in the direction of the small guide dimension, b

z is the principal axis in the longitudinal direction

The component fields for the TE_{10} Mode are

$$H_z = C \cos\pi x/a$$

$$H_x = \frac{j2aC}{\lambda_g} \sin\pi x/a$$

$$E_y = \frac{-j2aC}{\lambda_0} \sin\pi x/a \quad \text{where C is a constant.}$$

For small holes $E_{y1} = E_{y2}$; $H_{x1} = H_{x2}$; and $H_{z1} = H_{z2}$.

Omitting for the time being the exponential factor and substituting the above equations into equation (46).

$$A = j\frac{2\pi r^3}{3a^2b}\left(\frac{\lambda_g}{2a}\right)\left[\left(\frac{2a}{\lambda_0}\right)^2 \sin^2\frac{\pi x}{a} - 2\left(\frac{2a}{\lambda_g}\right)^2 \sin^2\frac{\pi x}{a} - 2\left(\cos^2\frac{\pi x}{a}\right)\right] \qquad (47)$$

factoring our $2a/\lambda_g$ gives

$$A = \frac{j2\pi r^3}{3a^2b}\left[\left(\frac{2a}{\lambda_0}\right)^2\left(\frac{\lambda_g}{2a}\right)\sin^2\frac{\pi x}{a} - 2\left(\frac{2a}{\lambda_g}\right)\sin^2\frac{\pi x}{a} - 2\left(\frac{\lambda_g}{2a}\right)\cos^2\frac{\pi x}{a}\right] \qquad (48)$$

Now making use of the identity, $\frac{1}{\lambda_0^2} = \frac{1}{4a^2} + \frac{1}{\lambda_g^2}$, λ_0 may be eliminated from the equation (48), leaving

$$A = j\frac{2\pi r^3}{3a^2b}\left[\left(\frac{\lambda_g}{2a} + \frac{2a}{\lambda_g}\right)\sin^2\frac{\pi x}{a} - \left(\frac{2a}{\lambda_g}\right)2\cdot\sin^2\frac{\pi x}{a} - \left(\frac{\lambda_g}{2a}\right)2\cos^2\frac{\pi x}{a}\right] \qquad (49)$$

This is the equation for determining the forward coupled voltage in a common guide wall of zero thickness. If this wall has a finite thickness, the electric term will have an attenuation coefficient, α_E, and the magnetic terms have an attenuation coefficient, α_H . This results in the following final equation which is used in the text:

$$A = j\,\frac{2\pi r^3}{3a^2 b}\left[\alpha_E\left(\frac{\lambda_g}{2a}+\frac{2a}{\lambda_g}\right)\sin^2\frac{\pi x}{a} - 2\alpha_H\left(\frac{2a}{\lambda_g}\right)\sin^2\frac{\pi x}{a} - 2\alpha_H\left(\frac{\lambda_g}{2a}\right)\cos^2\frac{\pi x}{a}\right] \quad (50)$$

with

$$\alpha_E = f(t,\lambda) \qquad t \text{ is thickness}$$
$$\alpha_H = f(t,\lambda)$$

The voltage coefficient due to the backward wave is developed in an identical manner, differing only in signs as indicated below.

$$B = j\,\frac{2\pi r^3}{3a^2 b}\left[\alpha_E\left(\frac{\lambda_g}{2a}+\frac{2a}{\lambda_g}\right)\sin^2\frac{\pi x}{a} + 2\alpha_H\left(\frac{2a}{\lambda_g}\right)\sin^2\frac{\pi x}{a} - 2\alpha_H\left(\frac{\lambda_g}{2a}\right)\cos^2\frac{\pi x}{a}\right] \quad (51)$$

APPENDIX B

THE DEVELOPMENT OF THE HOLE DIAMETERS FOR FORWARD VOLTAGE COUPLING COEFFICIENTS PROPORTIONAL TO TCHEBYSCHEFF POLYNOMIAL COEFFICIENTS

Dolph's method of computing the Tchebyscheff coefficients for an antenna with 2N elements can be applied to a directional coupler with 2N apertures or holes. These coefficients will be made proportional to the forward voltage coupling coefficients rather than the feed currents of an antenna array.

Selecting 2N as ten gives

$$F_{2N}(\theta) = \sum_{n=1}^{N} t_n' \cos(2n-1)\theta \tag{52}$$

$$= t_1' \cos\theta + t_2' \cos 3\theta + t_3' \cos 5\theta + t_4' \cos 7\theta + t_5' \cos 9\theta$$

The non-normalized Tchebyscheff polynomials for cos(2n-1) θ are for

$n=1, \quad \cos\theta = x$

$2, \quad \cos 3\theta = 4x^3 - 3x$

$3, \quad \cos 5\theta = 16x^5 - 20x^3 + 5x$

$4, \quad \cos 7\theta = 64x^7 - 112x^5 + 56x^3 - 7x$

$5, \quad \cos 9\theta = 256x^9 - 576x^7 + 432x^5 - 120x^3 + 9x$

Substituting these in (52) above

$$\begin{aligned} G_{2N-1}(x) = {} & t_1' x \\ & + t_2' 3x + t_2' 4x^3 \\ & + t_3' 5x - t_3' 20x^3 + t_3' 16x^5 \\ & - t_4' 7x + t_4' 66x^3 - t_4' 112x^5 + t_4' 64x^7 \\ & + t_5' 9x - t_5' 120x^3 + t_5' 432x^5 - t_5' 576x^7 + t_5' 256x^9 \end{aligned} \tag{53}$$

and then regrouping the terms gives

$$\begin{aligned} G_{2N-1}(x) = {} & 256\, t_5' x^9 \\ & + (-576\, t_5' + 64\, t_4') x^7 \\ & + (432\, t_5' - 112\, t_4' + 16\, t_3') x^5 \\ & + (-120\, t_5' + 56\, t_4' - 20\, t_3' + 4 t_2') x^3 \\ & + (9 t_5' - 7 t_4' + 5 t_3' + 3 t_2' + t_1') x \end{aligned} \tag{54}$$

The Tchebyscheff polynomial of order 2N-1 or 9, in Z_ox is

$$T_9(z_0x) = 256x^9z_0^9 - 576x^7z_0^7 + 432x^5z_0^5 - 120x^3z_0^3 + 9xz_0 \qquad (55)$$

Equating equations (54) and (55) by setting like coefficients of x equal gives

$$t_5' = z_0^9 \qquad (56)$$

$$t_4' = 9(t_5' - z_0^7) \qquad (57)$$

$$t_3' = -27(t_5' - z_0^5) + 7t_4' \qquad (58)$$

$$t_2' = 30(t_5' - z_0^3) - 14t_4' + 5t_3' \qquad (59)$$

$$t_1' = -9(t_5' - z_0) + 7t_4' - 5t_3' + 3t_1' \qquad (60)$$

The parameter, z_o, may be solved for by the following formula:

$$z_0 = \frac{1}{2}\left[(g + \sqrt{g^2-1})^{1/m} + (g - \sqrt{g^2-1})^{1/m}\right]$$

For g equal to 1500 and m equal to 9,

$$z_0 \simeq \frac{1}{2}\left[(2g)^{1/m} + (1/2g)^{1/m}\right] = 1.422$$

Substituting this value of z_o in equations (56) through (60), the non-normalized Tchebyscheff coefficients are obtained.

$t_5' = 20.60$

$t_4' = 91.05$

$t_3' = 225.16$

$t_2' = 387.69$

$t_1' = 501.51$

From these, the normalized coefficients are

$t_5 = 1.00$
$t_4 = 4.42$
$t_3 = 10.93$
$t_2 = 18.82$
$t_1 = 24.35$

These coefficients must now be placed equal to the forward coupling coefficients, A_n, where n goes from 1 to 10, corresponding to the holes of the ten coupling elements. t_5 was made proportional to A_1 and A_{10} because of symmetry.

$t_4 \propto A_2$ and A_9
$t_3 \propto A_3$ and A_8
$t_2 \propto A_4$ and A_7
$t_1 \propto A_5$ and A_6

For a -3 db coupler the holes corresponding to these coupling coefficients would be too large to conform with Bethe's small hole theory. Four ten element arrays with the voltage coefficients superimposed as shown in figure (7), were used.

Element	1	2	3	4	5	6	7	8	9	10	11	12	13	14	15	16	17	18	19	20	21	22
Array #1	t_5	t_4	t_3	t_2	t_1	t_1	t_2	t_3	t_4	t_5												
Array #2					t_5	t_4	t_3	t_2	t_1	t_1	t_2	t_3	t_4	t_5								
Array #3									t_5	t_4	t_3	t_2	t_1	t_1	t_2	t_3	t_4	t_5				
Array #4													t_5	t_4	t_3	t_2	t_1	t_1	t_2	t_3	t_4	t_5

Line of Symmetry

The value of the final T_n coefficients (where n is the total number of elements and now goes from 1 to 22) for a given element is the sum of the vertical column above the particular element to be computed.

Due to symmetry the following tabulation need be made only for eleven elements:

T_1	T_2	T_3	T_4	T_5	T_6	T_7	T_8	T_9	T_{10}	T_{11}
1.00	4.42	10.93	18.82	24.35	24.35	18.82	10.93	4.42	1.00	
				1.00	4.42	10.93	18.82	24.35	24.35	18.82
								1.00	4.42	10.93
1.00	4.42	10.93	18.82	25.35	28.77	29.75	29.75	29.77	29.77	29.75

The total sum of the 22 Tchebyscheff coefficients as modified by the superimposition is

$$T_T = 2\sum_{n=1}^{11} T_n = 476.16$$

For coupling of -3 db,

$$-3\,db = 20 \log A_T \;; \quad then\ A_T = 0.708$$

where A_T is the total of the voltage coefficients to be coupled.

Then by the simple relation $2 x T_T/T_n = A_T/A_n$, the voltage coefficient for hole n, A_n, was computed. The two in this relation is for the two rows of 22 elements.

The transcendental equation for A_n was plotted by assuming values of r_n. Then by computing the values of A_n from this equation, the radii of the 11 different sized coupling holes was obtained from this plot. For accuracy, the value of the radii obtained from the plot was substituted in the equation for A_n to check if the correct value of voltage was coupled.

TABULATION of A_n AND D_n

$A_1(A_{22}) = 7.426 \times 10^{-4}$	$d_1 = .121''$
$A_2(A_{21}) = 3.282 \times 10^{-3}$	$d2 = .184$
$A_3(A_{20}) = 8.117 \times 10^{-3}$	$d_3 = .240$
$A_4(A_{19}) = 1.398 \times 10^{-2}$	$d_4 = .282$
$A5(A_{18}) = 1.882 \times 10^{-2}$	$d_5 = .308$
$A_6(A_{17}) = 2.136 \times 10^{-2}$	$d6 = .320$
$A_7(A16) = 2.209 \times 10^{-2}$	$d_7 = .324$
$A_8(A15) = 2.209 \times 10^{-2}$	$d_8 = .324$
$A_9(A_{14}) = 2.211 \times 10^{-2}$	$d_9 = .324$
$A_{10}(A13) = 2.211 \times 10^{-2}$	$d_{10} = .324$
$A_{11}(A_{12}) = 2.209 \times 10^{-2}$	$d_{11} = .324$

JUL 2
FEB 8
MAR 11
NOV 24
4 MAY 71

BINDERY
889
RENEWED
DISPLAY
18600

Thesis
E27 Eidson 20753
A broad band bi-directional coupler with tight coupling and high directivity

FEB 8
MAR 11
4 MAY 71

BINDERY
889
RENEWED
DISPLAY
18600

Thesis
E27 Eidson 20753
A broad band bi-directional coupler with tight coupling and high directivity

Library
U. S. Naval Postgraduate School
Monterey, California

ARTISAN
GOLD LETTERING
AND
SMITH BINDERY
OAKLAND, CALIF

thesE27
A broad band bi-directional coupler with
3 2768 001 90374 3
DUDLEY KNOX LIBRARY